White Paper
SPRAB12–November 2008

Signal Processing Overview of Ultrasound Systems for Medical Imaging

Murtaza Ali, Dave Magee and Udayan Dasgupta

This white paper provides a description of ultrasound imaging systems with focus on the signal processing strategies. The different system components are briefly discussed followed by a description of ultrasound related peculiarities that the system needs to handle. The system processing for B-mode imaging can be roughly divided into three components: the front end (that includes transmission, reception, and digitization of ultrasound signal), followed by beamforming (to focus on a particular scan line), the mid end (that performs demodulation, envelope detection, and compression), and finally, the back end (that performs various image enhancement and rendering functions). The processing required in Doppler mode is described and, finally, the processing and issues related to 3D/4D imaging using ultrasound systems are briefly discussed.

Contents

List of Figures

List of Tables

1 Introduction

Ultrasound is one of the most widely used modalities in medical imaging. Ultrasound imaging is regularly used in cardiology, obstetrics, gynecology, abdominal imaging, etc. Its popularity arises from the fact that it provides high-resolution images without the use of ionizing radiation. It is also mostly non-invasive, although an invasive technique like intra-vascular imaging is also possible. Non-diagnostic use of ultrasound is finding increased use in clinical applications, (e.g., in guiding interventional procedures). There are also novel non-imaging uses of ultrasound like bone densitometer where the ultrasound speed difference is used to measure the depth or width of bones non-invasively.

Ultrasound systems are signal processing intensive. With various imaging modalities and different processing requirements in each modality, digital signal processors (DSP) are finding increasing use in such systems. The advent of low power system-on-chip (SOC) with DSP and RISC processors is allowing OEMs to provide portable and low cost systems without compromising the image quality necessary for clinical applications.

This white paper introduces ultrasound systems. The focus of this paper is on the signal processing aspects of the ultrasound system [20]. The basic concepts behind ultrasound systems are provided in Section 2. In this section, the components that a modern ultrasound system are based on are provided along with a brief description of ultrasound properties applicable to imaging. Section 3 introduces the ultrasound transducer that forms the basic ultrasound transmission and reception sensor for this imaging mode. Section 4 focuses on front-end processing with special attention to the basics of beamforming using multiple transducer elements. The most commonly used delay and sum (DAS) beamforming is also introduced in this section. Section 5 describes the mid-end processing, which is defined as any processing that is done on each scan line during image acquisition. Section 6 describes the back-end processing of an ultrasound system, which is composed of image enhancement, noise reduction, and display functionalities. Section 7 describes the Doppler mode of operation, which provides a visual display of motion inside the body. Finally, Section 8 briefly introduces the basic concepts used for 3D/4D imaging.

2 Ultrasound System: Basic Concepts

This section introduces basic ultrasound concepts to help you understand how ultrasound systems function and to provide a basis for algorithm discussion. This is, by no means, an exhaustive survey of ultrasound systems.

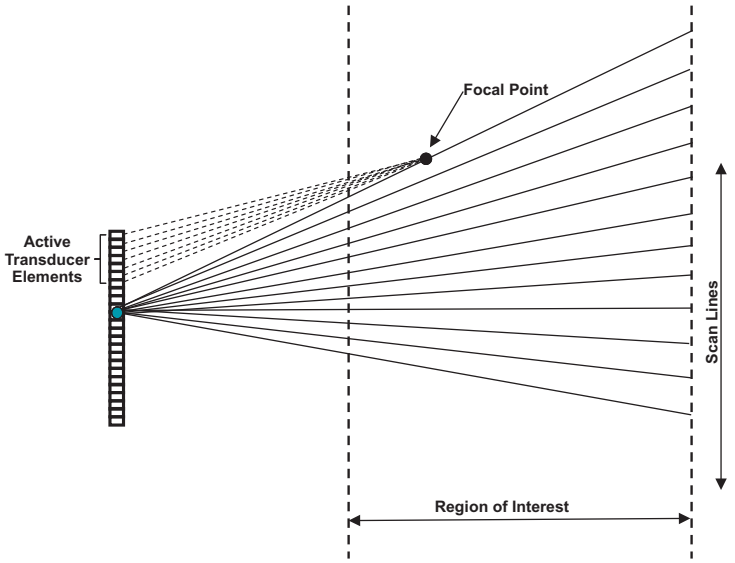

Figure 1. Ultrasound System – Sound Wave Focusing

2.1 Basic Functionality

Figure 1 shows the basic functionality of an ultrasound system. It demonstrates how transducers focus sound waves along scan lines in the region of interest. The term ultrasound refers to frequencies that are greater than 20 kHz, which is commonly accepted to be the upper frequency limit the human ear can hear. Typically, ultrasound systems operate in the 2 MHz to 20 MHz frequency range, although some systems are approaching 40 MHz for harmonic imaging [3]. In principle, the ultrasound system focuses sound waves along a given scan line so that the waves constructively add together at the desired focal point. As the sound waves propagate towards the focal point, they reflect off on any object they encounter along their propagation path. Once all of the reflected waves have been measured with the transducers, new sound waves are transmitted towards a new focal point along the given scan line. Once all of the sound waves along the given scan line have been measured, the ultrasound system focuses along a new scan line until all of the scan lines in the desired region of interest have been measured.

To focus the sound waves towards a particular focal point, a set of transducer elements are energized with a set of time-delayed pulses to produce a set of sound waves that propagate through the region of interest, which is typically the desired organ and the surrounding tissue. This process of using multiple sound waves to steer and focus a beam of sound is commonly referred to as beamforming. Once the transducers have generated their respective sound waves, they become sensors that detect any reflected sound waves that are created when the transmitted sound waves encounter a change in tissue density within the region of interest. By properly time delaying the pulses to each active transducer, the resulting time-delayed sound waves meet at the desired focal point that resides at a pre-computed depth along a known scan line. The amplitude of the reflected sound waves forms the basis for the ultrasound image at this focal point location. Envelope detection is used to detect the peaks in the received signal and then log compression is used to reduce the dynamic range of the received signals for efficient display. Once all of the amplitudes for all of the focal points have been detected, they can be displayed for analysis by the doctor or technician. Since the coordinate system, in which the ultrasound system usually operates, does not match the display coordinate systems, a coordinate transformation, called scan conversion, needs to be performed before being displayed on a CRT monitor.

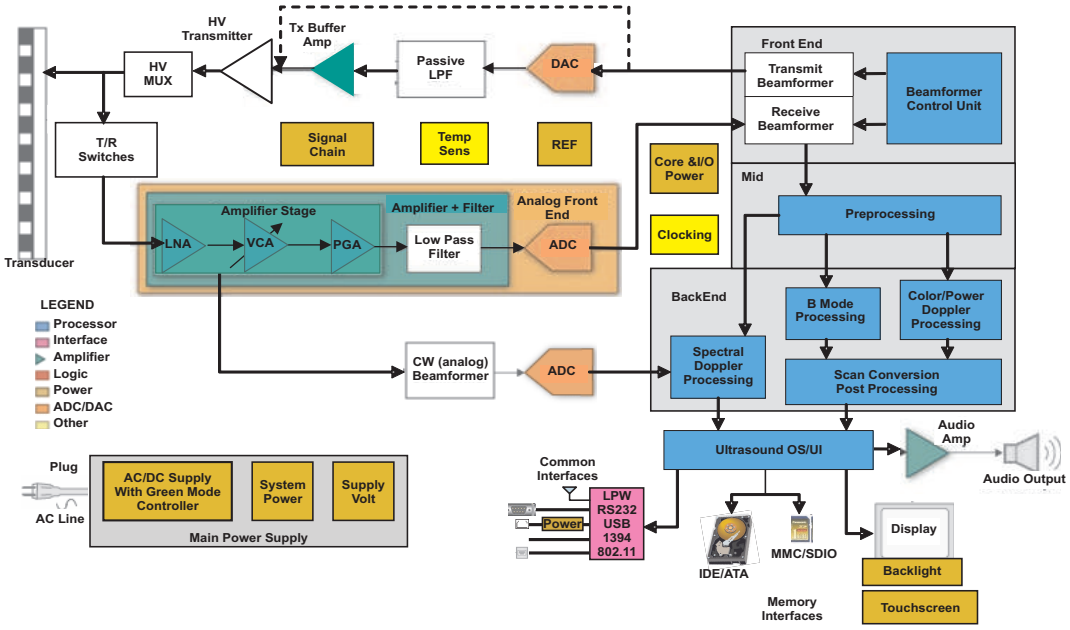

Figure 2. Ultrasound System Block Diagram

2.2 System Components

The system components are discussed in this section to provide a functional understanding of the system. The starting point for this discussion is the beamformer control unit shown in Figure 2, which is responsible for synchronizing the generation of the sound waves and the reflected wave measurements. The controller knows the region of interest in terms of width and depth. This region gets translated into a desired number of scan lines and a desired number of focal points per scan line. The beamformer controller begins with the first scan line and excites an array of piezo-electric transducers with a sequence of high voltage pulses via transmit amplifiers. Typical performance numbers for the amplifiers is ± 100 V and ± 2 Amps for each piezo-electric element. The pulses go through a transmit/receive (Tx/Rx) switch, which prevents the high voltage pulses from damaging the receive electronics. Note that these high voltage pulses have been properly time delayed so that the resulting sound waves can be focused along the desired scan line to produce a narrowly focused beam at the desired focal point. The beamformer controller determines which transducer elements to energize at a given time and the proper time delay value for each element to properly steer the sound waves towards the desired focal point.

As the sound waves propagate toward the desired focal point, they migrate through materials with different densities. With each change in density, the sound wave has a slight change in direction and produces a reflected sound wave. Some of the reflected sound waves propagate back to the transducer and form the input to the piezo-electric elements in the transducer. The resulting low voltage signals are scaled using a variable controlled amplifier (VCA) before being sampled by analog-to-digital converters (ADC). The VCA is configured so that the gain profile being applied to the received signal is a function of the sample time since the signal strength decreases with time (e.g., it has traveled through more tissue). The number of VCA and ADC combinations determines the number of active channels used for beamforming. It is usual to run the ADC sampling rate 4 times or higher than the transducer center frequency.

Once the received signals reach the Rx beamformer, the signals are scaled and appropriately delayed to permit a coherent summation of the signals. This new signal represents the beamformed signal for one or more focal points along a particular specific scan line. The beamformer operations are typically performed in application-specific integrated circuit (ASIC), field-programmable gate array (FPGA), DSP or a combination of these components. The choice of devices depends on the number of channels used in beamforming, which determines the input/output (I/O) requirement as well as the processing requirement to perform digital beamforming.

Once the data is beamformed, depending on the imaging modes, various processings are carried out. For example, it is common to run the beamformed data through various filtering operation to reduce out band noise. In B (Brightness) mode, demodulation followed by envelope detection and log compression is the most common practice. Several 2D noise reduction and image enhancement functions are also performed in this mode followed by scan conversion to fit the desired display system. In Doppler mode, the demodulation operation is followed by velocity and turbulence estimation. A color transformation is used to represent the velocity and turbulence and, finally, superimposed with B-mode imaging for display. In spectral mode, an windowed fast Fourier transform (FFT) is performed on the demodulated signal and displayed separately. It is also common to present the data on a speaker after separation of forward and reverse flow. Ultrasound systems designer has the choice of implementing these in FPGA, ASIC, DSP or a combination of these components. DSPs are gaining popularity due to their flexibility to implement these various algorithms along with their power efficiencies.

These systems also require good display capabilities since several different displays are usually overlaid for ease of diagnosis. Further, real-time control is a must for these systems. Therefore, modern SOCs that include DSP, RISC, graphics and video display systems are ideally suited for these systems where portability and low power are desired.

So far, this section has concentrated on digital beamforming, which is common for pulse wave (PW) based ultrasound systems. As described earlier, in these systems, a repeated set of pulse is sent through the transducer. In between the pulses, the received signal is recorded. There is an alternate mode where a continuous pulse sets are transmitted. These systems are known as continuous wave (CW) systems. These systems are used where a more accurate measurement of velocity information is desired using Doppler techniques. The disadvantage of this system is that it loses the ability to localize the velocity information. In these systems, a separate set of transducers are used for transmission and reception. Due to large immediate reflection from the surface of the transducer, the dynamic range requirement becomes very high to use ADC to digitize the reflected ultrasound signal and maintain enough signal to noise (SNR) for estimating the velocity information. Therefore, an analog beamforming is usually used for CW systems followed by analog demodulation. Such systems can then use lower sampling rate (usually in KHz range) ADCs with higher dynamic range.

2.3 Imaging Modes

This section discusses the various imaging modes found in today's ultrasound system.

- A-mode (Amplitude) imaging displays the amplitude of a sampled voltage signal for a single sound wave as a function of time. This mode is considered 1D and used to measure the distance between two objects by dividing the speed of sound by half of the measured time between the peaks in the A-mode plot, which represents the two objects in question. This mode is no longer used in ultrasound systems.
- B-mode (Brightness) imaging is the same as A-mode, except that brightness is used to represent the amplitude of the sampled signal. B mode imaging is performed by sweeping the transmitted sound wave over the plane to produce a 2D image. Typically, multiple sets of pulses are generated to produce sound waves for each scan line, each set of pulses are intended for a unique focal point along the scan line.
- For CW (Continuous Wave) Doppler, a sound wave at a single frequency is continuously transmitted from one piezo-electric element and a second piezo-electric element is used to continuously record the reflected sound wave. By continuously recording the received signal, there is no aliasing in the received signal. Using this signal, the blood flow in veins can be estimated using the Doppler frequency (see Section 7 for details). However, since the sensor is continuously receiving data from various depths, the velocity location cannot be determined.
- For PW (Pulse Wave) Doppler, several pulses are transmitted along each scan line and the Doppler frequency is estimated from the relative time between the received signals. Since pulses are used for the signaling, the velocity location can also be determined.
- For Color Doppler, the PW Doppler is used to create a color image that is super-imposed on top of B-mode image. A color code is used to denote the direction and magnitude of the flow. Red typically denoted flow towards the transducer and blue denotes flow away from it. A darker color usually denotes a larger magnitude while a lighter color denotes a smaller magnitude.

- In Power Doppler, instead of estimating the actual velocity of the motion, the strength or the power of the motion is estimated and displayed. It is useful to display small motion. There is no directional information in this measurement.
- Spectral Doppler shows the spectrum of the measured velocity in a time varying manner. Both PW and CW Doppler systems are capable of showing spectral Doppler.
- M-mode display refers to scanning a single line in the object and then displaying the resulting amplitudes successively. This shows the movement of a structure such as a heart. Because of its high pulse frequency (up to 1000 pulses per second), this is useful in assessing rates and motion and is still used extensively in cardiac and fetal cardiac imaging.
- Harmonic Imaging is a new modality where the B-mode imaging is performed on the second (or possibly other) harmonics of the imaging [3]. Due to the usual high frequency of the harmonic, these images have higher resolution than conventional imaging. However, due to higher loss, the depth of imaging is limited. Some modern ultrasound systems switch between harmonic and conventional imaging based on depth of scanning. This system imposes stringent linearity requirements on the signal chain components.
- Elasticity/Strain Imaging is a new modality where some measures of elasticity (like Young's modulus) of the tissue (usually under compression) is estimated and displayed as an image [17], [18]. These types of imaging have been shown to be able to distinguish between normal and malignant tissues. This is currently a very active area of research both on clinical applications and in real-time system implementation.

2.4 Ultrasound Specific Effects

In this section, a short description of some of the characteristics that ultrasound signal processing is designed to tackle are presented.

2.4.1 Speckles

Ultrasound wave goes through three types of scattering: specular, diffusive and diffractive [24].

- Specular scattering: This occurs when the scattering object is large compared to the wavelength. In this case, the reflection process can be approximated as an incident ray with the scattered wavefront following the shape of the object.
- Diffusive scattering: This occurs when the scattering object is small compared to the wavelength. The resulting scattering radiates in all directions with insignificant phase difference among reflections from the surface of the object.
- Diffractive Scattering: This occurs when the object size is in between the two extremes above.

A tissue is often modeled as an aggregate of small sub wavelength point scatters. The scattered signal from such an object is then the sum of many small reflections whose phase is uniformly distributed between 0 and 2π. By central limit theorem, the resulting signal can be viewed as a complex Gaussian random variable. Note that the detection of the signal is done non-coherently, only the envelope of the signal is used for imaging. The pixel intensity follows a Raleigh distribution. In the presence of a strong scattering object (specular scattering), the pixel intensity follows a Rician distribution. The impact of this shows up as 2D alternating regions of high and low intensity in the image. This effect is called *speckle*.

Speckles, though modeled with a distribution over the image, is not strictly a random process in the sense that the same object when imaged under the same conditions will create the exact same speckles. Therefore, the processing needed for speckles are different from those due to random noise like thermal effects. Specific processing is usually designed to reduce the effect of speckle or to make imaging operations (like boundary detection) robust in the presence of speckles.

Speckles depend on the distribution of point scatterers within the tissue and appear to provide visual differentiation in terms tissue texture. Domain experts are used to differentiate tissues based on such observed textures. There is debate in the ultrasound community as to whether speckles are friends or foes. In general, a quantification of desired speckle reduction is difficult to come up with.

2.4.2 Pulse Propagation Effect in Lossy Media

The pulse propagation can be modeled through the material transfer function (MTF) written as a function of frequency, *f*, and depth of penetration, *z*, in the following manner [24]:

$$MTF(f,z) = exp(\gamma(f)z) \quad (1)$$

$$\gamma(f) = -\alpha(f) - i\beta(f) \quad (2)$$

$$\alpha(f) = \alpha_0 + \alpha_1 |f|^y \quad (3)$$

$$\beta(f) = k_0(f) + \beta_E(f) \quad (4)$$

where $k_0 = 2\pi f / c_0$, c_0 being the velocity of sound usually taken at the center frequency of the spectrum, $\beta(f)$ is an excess dispersion term resulting in frequency dependent phase velocity, and $\alpha(f)$ is the frequency dependent attenuation following power law (α_0, α_1, and y are constants).

If a pressure $P_0(f)$ is applied at depth $z = 0$, the pressure at any depth z is then given by:

$$P(f,z) = P_0(f)MTF(f,z) \quad (5)$$

The inverse Fourier transform of $MTF(f, z)$ can be used to determine an equivalent time response at any depth. Based on this, the following characteristics can be derived:

- Signal attenuates exponentially with distance and frequency. It is usually considered to be 1 dB per MHz per cm in tissues. However, the attenuation is low (0.2 dB per MHz per cm) in blood.
- Velocity dispersion, though small, may need to be considered for wideband signals as is the case of modern ultrasound transducers.
- In time domain, the signal response broadens with depth. At shorter distance, response is impulse like and with depth, it spreads over time.
- In frequency domain, there is a slight downward shift of peak in the resulting frequency spectrum with depth of penetration when a shaped (e.g., Gaussian) pulse is applied.

3 Transducers

This section focuses on current ultrasound transducer technology.

3.1 Current Architecture

Ultrasound systems today rely on the electro-mechanical properties of piezo-electric elements to generate the sound waves and to measure the amplitude of the reflected waves. These elements convert high voltage pulses into sound waves that travel through the relevant tissues during transmission and convert small displacements into small voltage waveforms during reception. These devices are quite expensive to manufacture because of the various layers that must be attached to achieve the desired level of impedance matching between the device and the human skin.

Figure 3. Ultrasound Transducer Types

The transducers come in a variety of shapes, each containing a specified number of piezo-electric elements. The application usually determines the type and size of the transducer. There are three main types of transducer: linear, curved, and sector as shown in Figure 3. Linear transducers are used primarily for small parts requiring high resolution and typically involve shallow depths. To achieve high resolution, higher frequencies are typically required. Since the elements are arranged in a linear fashion, the resulting image is rectangular. To broaden the field of view, sector transducers are used. These transducers have a small footprint and are good for cardio applications due to small rib spacing. For abdominal viewing, curved transducers are typically used because of resolution and penetration benefits. They allow for the maximum field of view and depth because of their large aperture. Note that any type of transducer can be phase arrayed to produce a beam of sound that can be steered and focused by the ultrasound controller.

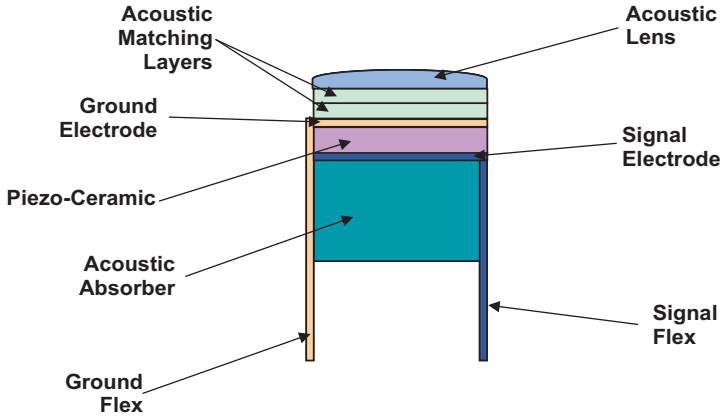

Figure 4. Ultrasound Transducer Cross-Sectional View

Figure 4 shows a cross-section of a conventional transducer. The signal flex and ground flex provide a connection from each piezo-electric element to ultrasound system. On one end, the signal flex is usually soldered to a group of wires in a cable bundle that is connected to the system via a standardized connector (e.g., ZIF156). This cable can become quite stiff for large element transducers. On the other end, the signal flex and the ground flex are connected to the signal and ground electrodes that are attached to the piezo-ceramic material. An acoustic absorber is attached to the back of the piezo-ceramic material to prevent any sound waves from the back of the transducer from interfering with the sound waves on the front of the transducer. Matching layers are attached to the front of the transducer in an attempt to match the acoustical impedance of the piezo-ceramic and the tissue of interest. Since the acoustical impedance for piezo-ceramics is around 20 to 30 MRayls and the human body is around 1.5, the matching layers try and achieve an average value of 6 to 7 MRayls. Since there are no known materials with this impedance level, multiple layers are used to achieve an equivalent impedance in this range. The matching layers are typically glued onto the ceramic material and then machined to control the thickness. This process is very time consuming and can be very expensive. After applying the matching layers, a lens is attached to the transducer to help focus the sound waves at the desired location.

The manufacturing of current ultrasound transducers is quite time consuming and expensive for several reasons. Many layers are glued together, which means that each surface must be properly prepared. Also, each glue interface must not contain air voids because they tend to scatter the sound waves as they propagate through each layer. Finally, all of the signals must be connected to transducer cable that connects to the main ultrasound system. Great care is taken to impedance match all of the piezo-electric element/wire pairs to ensure that all of the A/D converters see the same load. To avoid these issues, alternate transducer structures using capacitive micro-machined ultrasound transducers (CMUTs) is an active area of research [33].

4 Front-End Processing

This section describes the front-end signal processing that occurs in an ultrasound system.

4.1 Beamforming

As indicated in Section 2.1, the process of steering and focusing the sound beam in an ultrasound system is commonly referred to as phased array beamforming [26]. In this mode of operation, multiple piezo-electric elements are excited with properly time-delayed pulses and then become sensors to record the reflected sound waves. Figure 5 is used to explain how the time-delay values for each piezo-electric element is calculated. Notice that the location of the focal point in this figure is referenced using polar coordinates, but Cartesian coordinates could be used as well.

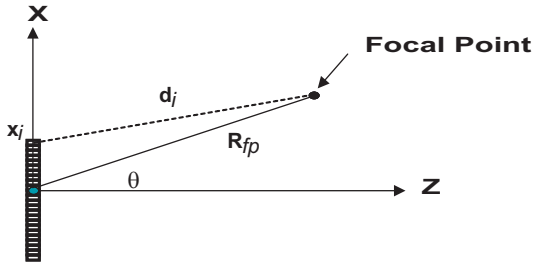

Figure 5. Focal Point Representation - Polar Coordinates

Suppose that each piezo-electric element is driven with the same pulse waveform, *p(t)*. The propagation time, t_i, for the *ith* piezo-electric element to the focal point can be written as:

$$t_i = \frac{\sqrt{R_{fp}^2 + x_i^2 - 2x_i R_{fp} \sin(\theta)}}{c} \tag{6}$$

where x_i is the x-axis coordinate of the ith piezo-electric element, R_{fp}, is the radial distance from the origin to the focal point, θ, is the angle of the focal point with respect to the z-axis, and *c* is the speed of sound. Notice that θ defines the scan line of interest. In general, multiple focal points are analyzed for a given scan line that makes R_{fp} a function of time.

To ensure that the sound waves from each piezo-electric element arrive at the focal point at the same time, the pulse waveform to each element must be delayed by this amount. By studying Equation 6, the maximum propagation time for a given (R_{fp}, θ) configuration (i.e., focal point) becomes:

$$t_{max} = \frac{\sqrt{R_{fp}^2 + x_{max}^2 + 2x_{max}R_{fp} \sin(\theta)}}{c} \tag{7}$$

This value is used to bias the time-delay values so that the pulse start time for the piezo-electric element that is furthest away from the focal point is time zero. Therefore, the pulse waveform for the *ith* piezo-electric element becomes:

$$p_i(t) = p(t - \tau_i) \tag{8}$$

where $\tau_I = t_{max} - t_i$

Once the sound waves reach the focal point, some of the sound waves will reflect back towards the transducer. One can assume that the focal point is emitting a sound wave and the transducer is recording the received sound wave at each piezo-electric element. As a result, the propagation time from the focal point back to the *ith* piezo-electric element is the same value as that given in Equation 6. The received signal, *r(t)*, from a given focal point after it has been time ligned can be written as:

$$r(t) = \sum_{i=1}^{N} A_{ri} \sum_{j=1}^{N} A_{tj} p\left(t - \tau_{ri} - \tau_{tj}\right) \tag{9}$$

where A_{ri} is the apodization applied to each receive signal, A_{tj} is the apodization applied to each transmit signal, τ_{ri} is the time-delay value applied to each received signal, and τ_{tj} is the time-delay value applied to each transmitted signal. The apodization factors are used to shape the transmitted beam and to weight the received signals. Sidelobes can be dramatically reduced by properly adjusting these factors.

The process of beamforming can be broken down into two main components: steering and focusing. Steering is performed by adjusting the angle, θ, which controls the direction of the beam and focusing is performed at various time intervals along a given scan line. An efficient implementation will have the largest ΔR_{fp} possible so that multiple image points can be retrieved for a single pulse sequence to the piezo-electric elements. Unfortunately, Equation 6 cannot be separated into terms that just depend on R_{fp} and θ. One common solution is to approximate this equation with a Taylor series expansion that yields:

$$t_i \approx \frac{R_{fp} - \sin(\theta) x_i + \frac{\cos^2(\theta)}{2R_{fp}} x_i^2}{c} \tag{10}$$

This second order approximation minimizes the mean squared error for the values of R_{fp} under consideration. Peak errors are less than 1/8 wavelength. Other approximations can also be used [28].

The linear term,
$-\frac{\sin(\theta)}{c} x_i$,
is often referred to as the beamsteering component because it only depends upon θ and is fixed over all the focal points along a particular scan line. The quadratic term,
$\frac{\cos^2(\theta)}{2cR_{fp}} x_i^2$,
is referred to as the dynamic focusing component because it depends on the focal point and can be used to adjust the focal point of the received data from the piezo-electric elements. Also notice that $x_1 = i\,\Delta x$, where *i* is the channel number and Δx is the piezo-electric element spacing. Therefore, these terms can be easily expressed in terms of channel number for easy implementation.

5 Mid-End Processing

The term *mid-end processing* does not have any common definition. The exact demarcation between mid-end and back-end processing is difficult to make. For this discussion, *mid-end processing* is defined to be any signal processing that occurs only on a single scan line of beamformed RF data at a time. Any 2D processing is considered as back-end processing.

5.1 Baseline Processing

There are some essential signal processing functions that each of the conventional ultrasound systems perform. These include filtering, detection, and log compression (see Figure 6). These operations are briefly described in the following subsections.

Figure 6. Basic Mid-End Processing

5.1.1 Filtering

This is typically band-pass filtering to reduce noise outside frequencies of interest. Another function of the band-pass filter is to select whether imaging is done on the fundamental frequency (conventional imaging) or the second harmonic (harmonic imaging). The selection could be done by the operator or automatically based on the depth of measurements. Fundamentals have better penetration and are selected when imaging is done deeper into the body. However, harmonic imaging has better resolution due to higher frequency operation and better tissue distinguishing properties.

5.1.2 Detection

Ultrasound imaging is typically done non-coherently on the envelope of the signal. This envelope extraction process is commonly called *detection* in ultrasound terminology. The first stage in this process is to get a complex signal using any of the following methods.

- An analytic representation of the signal is created via Hilbert transform. The advantage of this operation is that it is independent of the actual frequency of the operating frequencies and independent of the imaging mode (conventional versus harmonic), or changes in the center frequencies with time (e.g., a physical phenomenon in the tissue that results in a change of frequency with the depth of penetration). However, this operation is more complex compared to the alternative below.
- A complex rotator is used to demodulate the signal in baseband followed by low pass filtering to eliminate sidelobes. This operation is simpler and appears to be choice for implementation. However, the operating center frequency needs to be known and possibly tracked for changes.

The magnitude of the resulting complex signal is then used as detected signal for imaging. Additional low pass filtering with decimation or interpolation may be carried out on this signal before presenting this for further processing to bring the amount of data in line with display properties.

5.1.3 Log Compression

The maximum dynamic range of the human eye is in the order of 30 dB [24]. The actual dynamic range of the received signal depends on the ADC bits, the TGC amplifier used in the front end, and the depth of penetration. The signal is compressed to fit the dynamic range used for display (usually 7 or 8 bits). It is typical to use a log compressor to achieve the desired dynamic range for display. Some parameters in the compression function can be used to adjust brightness.

5.2 Advanced Signal Processing

Some advanced signal processing algorithms that are found in literature are described in this section.

5.2.1 Matched Filtering

This applies to the case of coded excitation [16]. The coded excitation is used to increase the depth of penetration and increase sensitivity without increasing the transmit pulse power, or equivalently, the ultrasound pressure. It is useful to improve the depth of penetration within the safety rules of operation. Two types of coded excitation have been reported in literature.

- Coded excitation: Several coded sequences like Barker and Golay sequences [10] have been used.
- Chirps: This is borrowed from radar where the transmit waveform consists of a linear sweep of frequency modulated pulse of a given duration [11].

As is clear from the choice of coded sequences, they are designed to provide an impulse like auto-correlation properties. If a coded excitation is used, then the received signal need to be filtered through the corresponding matched filter (or sequence).

5.2.2 Time Frequency Compensation (TFC)

To reduce the effect of changing center frequency with the depth of penetration, additional processing can be done to improve performance. The most common is changing center frequency of band-pass filter with time. The processing may also include some sort of estimation of frequency offset with the time of collection of data.

5.2.3 Frequency Compounding

This process reduces the speckles inherent in ultrasound imaging. The idea is to divide the signal before detection into overlapping frequencies via a multiple of band-pass filtering. The output of each of the filters is then individually detected and log compressed as mentioned earlier. Finally, they are weighted and added [24]. This is illustrated in Figure 7.

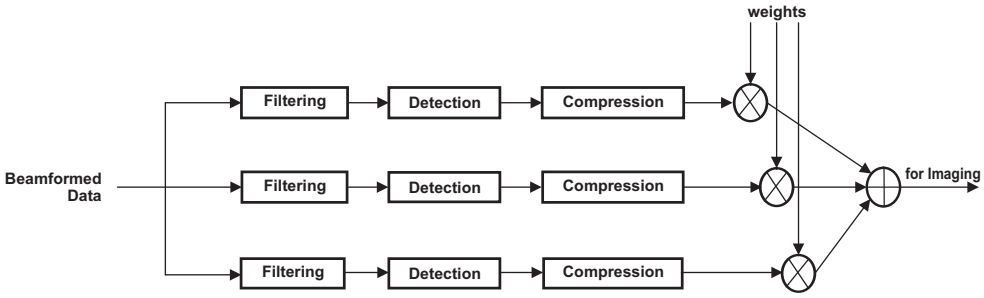

Figure 7. Frequency Compounding

Since speckles occur due to in-phase and out-of-phase distribution of the received ultrasound beam, the operations in frequency compounding have the effect of decorrelating the phase. The resulting non-coherent detection of individual signals had speckles that are decorrelated, and when summed, results in reduced overall speckle effect.

5.2.4 Axial and Lateral Gain Control

The time gain control (TGC), usually applied using the VCA as mentioned in Section 2.2, takes care of gain variation in the axial direction due to ultrasound signal attenuation. This signal attenuation is considered to be constant. However, the signal attenuation is dependent on anatomy. The attenuation could be low in anechoic regions like large fluid filled areas (e.g., gall bladder). In such cases, it is common to provide additional gain compensation both in the axial and lateral directions [15], [25]. These gain compensations can be under user control, but it is also possible to automatically detect such anechoic regions and provide an automatic gain control (AGC) mechanism.

Other uses of axial and lateral gain control include adjustment of signal due to loss in a region caused by shadowing of other structures like ribs and lungs, and allowing the physician to better visualize certain parts of the image.

5.2.5 Echo Line Averaging

Averaging over time is a useful technique to reduce noise and improve signal to noise ratio. In ultrasound systems, this can be performed by averaging in echo line. Usually an finite impulse response/infinite impulse response (FIR/IIR) filter can be run in time domain for every pixel in the echo line. Take care to include the effect of motion from frame to frame. One way to include the motion effect is to make the filter coefficients adaptive to changes to pixel values. For example, a single tap motion adaptive IIR filtering can be implemented using Equation 11 [22]:

$$y(i) = \frac{1}{1+\alpha}\left(x(i) + \alpha(i)y(i-1)\right),$$
$$\alpha(i) = f\left(\left|x(i) - y(i-1)\right|\right) \quad (11)$$

Here, *y(I)* is the output pixel value at time *I*, *x(I)* the input pixel value, and *f* is a monotonically decreasing function taking a value between 0 and 1. This is also sometimes known as persistence processing.

6 Back-End Processing

To form the best quality ultrasound images, it is often necessary to do a wide variety of operations before displaying the information for human observation. The exact processing and their order depend on the overall system configuration and the processing that has occurred at other parts of the system. This section provides a brief description of various operations performed before an image is considered ready for display.

6.1 Scan Conversion

The basic problem of scan conversion is to interpolate raw data to displayed data. The raw data can be in Cartesian coordinate (for linear probes) or in polar coordinates (for curvilinear or phased array probes). A coordinate transformation is needed to interpolate the data accurately on the display depending on the display resolution. Figure 8 shows an example of scan conversion from polar to Cartesian coordinate typical of ultrasound systems.

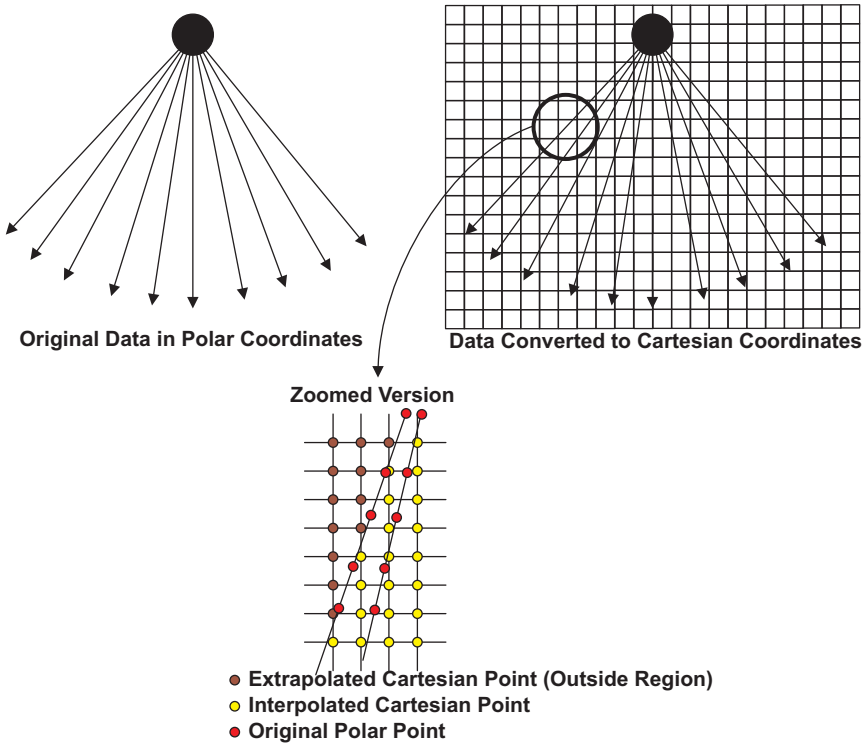

Figure 8. Scan Conversion

Typically, the algorithm computes the interpolated points based on their neighbors. Bilinear interpolation is the most commonly used technique for scan conversion. Typical systems use linear interpolation based on four nearest neighbors (2 X 2 interpolation). Some high-end systems may use interpolation based on 16 nearest neighbors (4 X 4 interpolation).

6.1.1 Angle (Spatial) Compounding

This is a multi-image method used for speckle reduction [24]. The idea is that by combining views of the same object from different angles, each having an uncorrelated speckle realization, the resulting image will have significantly reduced speckle. It operates by taking multiple views of the object, compensating them for translation/rotation (involves multiplying with a 2D matrix) and then obtaining their weighted combination to create the composite image.

Figure 9 illustrates the use of angle compounding, also known as spatial compounding. The image is acquired at different angles (illustrated as +20°, 0° and -20°). The final image is then averaged using some weighting function. Angle compounding also serves as sharpening the edges. The edges in ultrasound images are sharp when they are perpendicular to the scan line and they become somewhat blurry when the scan line is parallel to the edge (due to less reflection); therefore, imaging at multiple angles allows better viewing of the edges.

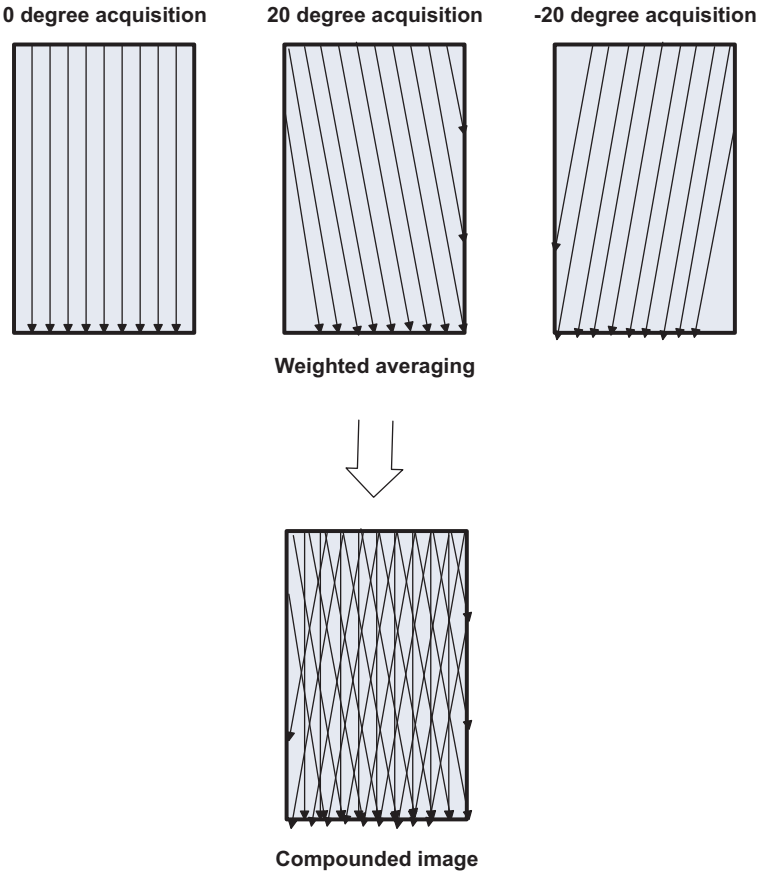

Figure 9. Angle Compounding

6.1.2 Frame Smoothing

Approaches to image smoothing include mask-based processing. Such processing uses neighbors of each pixel to generate a modified value for that pixel and is characterized by a weight mask on the pixels.

Table 1. Typical 3x3 Mask

w(-1,-1)	w(-1,0)	w(-1,1)
w(0,-1)	w(0,0)	w(0,1)
w(1,-1)	w(1,0)	w(1,1)

Typically masks such as that given in Table 1 are used in conjunction with Equation 12 to generate the processed image.

$$g(x,y) = \sum_{s=-a}^{a} \sum_{t=-b}^{b} w(s,t) f(x+s, y+t) \tag{12}$$

One way to smooth an image using mask-based techniques is a lowpass filter. A common side effect of this operation is unwanted blurring of features. Table 2 and Table 3 show masks for two lowpass filters that provide different smoothing/blurring characteristics [1].

Table 2. *Box* Filter Used for Smoothing – Often Causes Blurring

1	1	1
1	1	1
1	1	1

Table 3. Filter Used for Smoothing But Reduces Unwanted Blurring

1	2	1
2	4	2
1	2	1

Median filters (called order statistic filters) are also used as smoothing filters. These are statistical nonlinear filters often used to reduce noise without blurring the edges. They operate by first putting the neighboring pixels (indicated by a mask) into a sorted list and then choosing the middle value (median) as the output of the operation. Median filters perform poorly in extremely noisy cases (since the median value is a noise sample) and in presence of additive white Gaussian noise (AWGN).

Gaussian Filters are also used for smoothing. It is a separable filter as shown below and can be implemented using windows of length M = 3 σ or M = 5 σ.

$$h(x,y) = g_{2D}(x,y) = \left(\frac{1}{\sqrt{2\pi}\sigma} exp\left(-\frac{x^2}{2\sigma^2}\right)\right) \cdot \left(\frac{1}{\sqrt{2\pi}\sigma} exp\left(-\frac{y^2}{2\sigma^2}\right)\right), \\ = g_{1D}(x) \cdot g_{1D}(y) \quad (13)$$

6.1.3 Boundary/Edge Detection

A common method for edge detection uses sharpening filters that help in de-blurring an image. There are three main types of such filters: highpass filters, high-boost filters and derivative filters.

- Highpass filters: Typically, masks for these filters have positive values at the center and negative values towards the edges. One example is given in Table 4 [1].

Table 4. Typical Highpass Filter

-1	-1	-1
-1	-9	-1
-1	-1	-1

  The problem of highpass filters is that these filters often remove most of the information from the images except for the edges and, thereby, degrade the overall image quality.
- High-boost filters: These filters are weighted combination of original image and highpass filtered image, but the weights are often determined by trial-error. This technique is also known as unsharp masking [1].
- Derivative filters: These filters use an approximation of the 2D derivatives to sharpen the image. The derivative is given in Equation 14.

$$|\nabla f| = \sqrt{\left(\frac{\partial f}{\partial x}\right)^2 + \left(\frac{\partial f}{\partial y}\right)^2} \cong \left|\frac{\partial f}{\partial x}\right| + \left|\frac{\partial f}{\partial y}\right|, \quad where$$

$$\frac{\partial f}{\partial x} = f(x,y) - f(x-1,y) \quad and \quad \frac{\partial f}{\partial y} = f(x,y) - f(x,y-1) \quad (14)$$

  However, it has the same issues as highpass filters and often need to be used within a high-boost filter framework.

6.1.4 Speckle Reduction

There are various approaches to speckle reduction that use multi-image approaches like frequency and angle compounding that was covered earlier in this document. For single-image approaches, median filtering (discussed in Section 6.1.3) or its extension known as adaptive median filtering, can be used to reduce speckles [13]. However, new approaches to speckle reduction have been reported in literature; the three main categories of speckle reduction techniques are briefly described here. The common themes of all these techniques are non-linear filtering and local statistics-based adaption.

- Non linear filtering: They provide edge preserving filtering while trying to smooth out noise.
- Local statistics based adaptation: Some statistics based on neighboring pixels are calculated and used to modify the filtering parameters.

6.1.4.1 Multi-Scale or Wavelet Decomposition With Soft Thresholding

Wavelet decomposition of an image allows multi-scale analysis of an image. A typical wavelet decomposition provides a hierarchical frequency division of the signal. This is represented in Figure 10. After each filtering, a down-sampling can be carried out to maintain Nyquist rate at each scale. It is usually a trade off between reconstructed image quality and processing requirements to decide whether down-sampling at each stage is carried out or not.

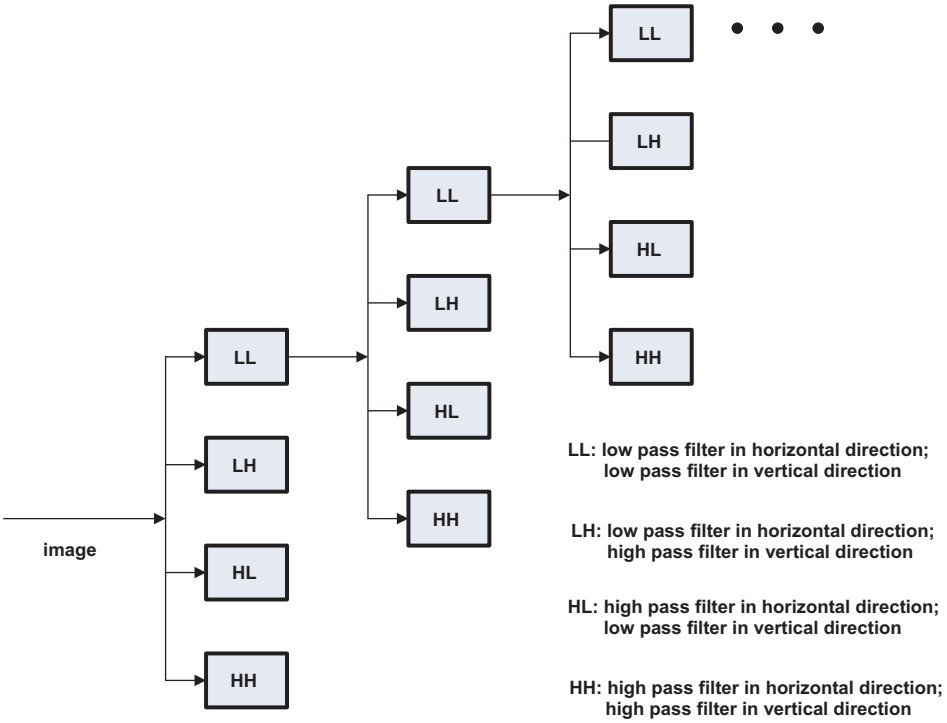

Figure 10. Wavelet Decomposition of an Image

Once the image representations at different scales are obtained, the transformed coefficients can be analyzed and different soft thresholding strategies can be applied, depending on both the local signal statistics at each scale and the scale itself [9], [34]. Lower scales preserve the low frequency components and more smoothing can be applied. The higher scales preserve the edges and directional smoothing can be applied there. The overall process with multi-scale soft thresholding is represented in Figure 11.

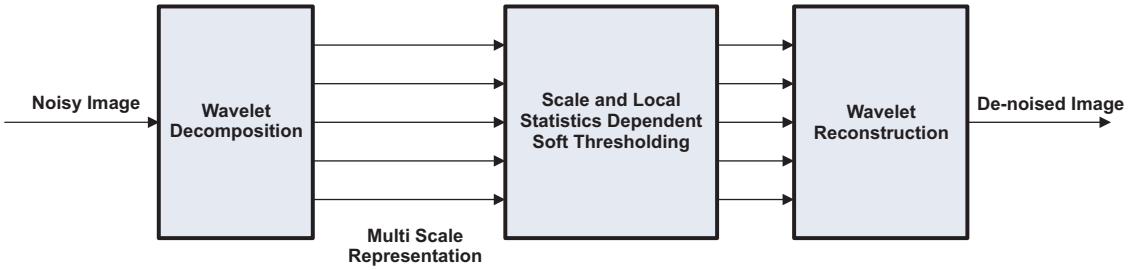

Figure 11. Soft Thresholding With Wavelet Decomposition

6.1.4.2 *Anisotropic Filtering*

The anisotropic filtering starts with a generalized non-homogeneous partial differential equation mimicking the physics of a diffusion process [2], [30].

$$\frac{\partial f}{\partial t} = \nabla \bullet \left(D\left(|\nabla f| \right) \nabla f \right) + \alpha s \tag{15}$$

Here $f = f(x, y, t)$ is the image at time instant t in the diffusion process, with the initial condition $f(x, y, 0)$ representing the original noisy image. $s = s(x, y, t)$ is a source term added to generalize the original diffusion equation and α is simply a weighting factor. s is usually derived from f. ∇ is the gradient operator with respect to spatial coordinates (x, y). $D()$ is a diffusion constant dependent on the local gradient.

At steady state of the process, the function f (i.e., the solution of this equation with the initial state being the noisy image) represents the smoothed image. The diffusion process can be controlled via the diffusion constant. The process will be isotropic when $D()$ is a constant (i.e., diffusion occurs in all radial directions in the same rate). For speckle reduction in ultrasound, we use anisotropic diffusion where $D()$ is a function of the gradient. In this way, the diffusion is dependent on whether there is an edge or not. $D()$ defines both the smoothing and the edge preserving aspects of the process. Common functions of $D()$ are given below (k being a constant):

$$D(s) = \frac{1}{1 + \left(\frac{s}{k} \right)^2}$$

$$D(s) = exp\left[-\left(\frac{s}{k} \right)^2 \right] \tag{16}$$

For practical implementation, the diffusion equation needs to be discretized. This results in an iterative filtering operation. Based on a suitable stoppage criterion, the final speckle reduce image is achieved after a number of iterations.

Anisotropic filtering can also be combined with multi-scale decomposition (e.g., wavelet decomposition) [30]. This provides the additional ability to choose the diffusion process through scale dependent choice of $D()$.

6.1.4.3 Bilateral Filtering

Bilateral filtering is introduced by Tomasi and Manduchi in 1998 [27]. A typical bilateral filtering in digital domain can be represented by:

$$\hat{f}(\vec{p}) = \sum_{\vec{q}} g_{\sigma s}\left(\left\|\vec{p}-\vec{q}\right\|\right) g_{\sigma r}\left(\left|f(\vec{p})-f(\vec{q})\right|\right) f(\vec{q}),$$

$$g_{\sigma}(x) = \frac{1}{\sqrt{2\pi}\sigma} exp\left(-\frac{x^2}{2\sigma^2}\right). \quad (17)$$

$g_{\sigma}(x)$ is the typical Gaussian filtering kernel. Here, $f(\vec{p})$ is the input pixel intensity at location $\vec{p}$, and $\hat{f}(\vec{p})$ is the filtered pixel intensity. The bilateral filtering operation consists of two kernels:

- The spatial filtering kernel, represented by $g_{\sigma s}$,provides more weight to nearby pixels and less to far away pixels.
- The range filtering kernel, represented by $g_{\sigma r}$, provides more weight to pixels whose intensities are close and less weight to pixels whose intensities differ widely.

A variation of bilateral filtering with very good properties was introduced by Zhang and Allebach [32], where the range kernel is modified to include a local statistics dependent parameter, $\xi(\vec{q})$

$$\hat{f}(\vec{p}) = \sum_{\vec{q}} g_{\sigma s}\left(\left\|\vec{p}-\vec{q}\right\|\right) g_{\sigma r}\left(\left|f(\vec{p})-f(\vec{q})-\xi(\vec{q})\right|\right) f(\vec{q}). \quad (18)$$

Several local statistics, based on the difference between the current pixel value and the mean around this pixel value, have shown to produce excellent noise reduction capability while preserving edges.

6.1.5 Histogram Equalization

This algorithm is typically used to improve image contrast and quality, and involves doing a gray level transformation to obtain a uniform histogram from images with un-balanced histograms. First, It computes the histogram of the image, then generates the cumulative density function (cdf). It then computes the modified pixel values as:

$$s(x,y) = round((cdf(r(x,h)) - cdf_{min})/(M \cdot N - cdf_{min}) \cdot (L-1)) \quad (19)$$

where *MxN* is the original image size and L is the number of gray scale levels.

6.1.6 Display Mode Dependent Processing

There is a significant amount of data processing that is not signal processing in nature, but plays a critical role in generating a superior image on the screen. Often these methods are vendor specific. They typically include a user-selectable look-up table (non-linear mapping) to convert echo amplitudes to display brightness or color. Careful choice of this parameter is important for best image display and strongly interacts with ambient lighting. This is also the stage where different kinds of information (B-mode, color Doppler, and color flow imaging) are combined for simultaneous display. Typically, support for user-actions (e.g., on-screen menus selections, zoom, etc.) are also provided in this module.

7 Doppler Processing

Doppler ultrasound and imaging are focused on measuring and displaying blood flow in the body. Images of blood circulation (color flow imaging or CFI), precise continuous wave (CW), and pulsed wave (PW) Doppler measurements are available on many systems.

Doppler effect is the shift in sound frequency as the source moves with respect to the observer. The governing equation for these measurements is [23]:

$$f_D = \Delta f = [2(V/c_0)\cos\theta] \cdot f_0, \quad (20)$$

where f_D= Doppler shift, C_0 = Speed of sound in intervening medium, V = Speed of object, θ = Angle of observation and f_0 = Frequency of measuring signal.

Details about different types are Doppler processing are discussed in the following sections.

7.1 Continuous Wave (CW) Doppler

The classic CW Doppler system is completely analog and has high sensitivity and selectivity, and is still used today. The probe is usually split in two halves (TX and RX). The demodulated received signal can be used to estimate velocities [8]. This data can be used for spectral display where the spectrum of the data is continuously displayed and updated. Since the data is in audible range, it can be sent to audio equipment after separation of forward and reverse flow Equation 6. A sampling rate change is also needed to change the sampling rate of the demodulated signal to that of the audio digital-to-analog converter (DAC) on the system.

7.2 Pulsed Wave (PW) Doppler

This overcomes the range ambiguity inherent in CW Doppler. PW Doppler sends pulses of a certain length to a target at a certain range. The received pulses are dilated (or contracted) due to Doppler, and hence, the delay in the arrival of the pulse also provides velocity information. In CW Doppler, the received frequency is compared to the transmitted frequency but in PW Doppler each received echo is compared to a similar echo from a previous transmission. The spectral Doppler display could be done similar to CW Doppler. Again the display typically also involves color flow imaging. The CFI image indicates pulse length, range depth and direction. Also both PW and CW processing involves a high pass filter (wall filter) to remove effects of slowly moving vessel/tissue walls. For PW processing, one needs to also use a LPF (Nyquist filter) with cutoff at $f_{Pulse\_Rep\_Freq}/2$ to remove aliasing effects [23].

7.3 Color Flow Imaging

Color flow imaging, using PW Doppler setup, provides real-time display of blood velocity and direction. The mean frequency is computed from N received samples using an autocorrelation-based method [7], [14]. For more information regarding the more common method developed by Kasai et al., see [7]. The mean velocity is given by,

$$\bar{v} = \frac{\bar{w}}{w_0} \cdot \frac{c}{2\cos\theta}$$

where W_0 is the carrier frequency, C is the velocity of sound, θ is the angle between sound beam and blood flow, and

$\bar{w}$

is the mean angular frequency of the power spectrum of the received signal.

Typically, flow direction is obtained from the polarity of the Doppler frequency shift. The turbulence of blood flow is measured by the variance.

$$\sigma^2 = \overline{w^2} - (\bar{w})^2 \quad (21)$$

The mean angular frequency and its variance can be found using the autocorrelation function of the complex input signal, $z(t)$. The mean angular frequency is calculated from the following equations:

$$\bar{w} = \frac{\phi(T)}{T} \text{ and } \phi(T,t) \tan \frac{R_y(T,t)}{R_x(T,t)} \quad (22)$$

And, its variance is calculated from:

$$\sigma^2 = \frac{1}{T^2}\left\{1 - \frac{|R(T)|}{R(0)}\right\} \tag{23}$$

For received complex signal, *z(t)*, the autocorrelation is expressed as:

$$R(T,t) = \int_{t'=t-nT}^{t'=t} z(t').z^*(t'-T)dt' = R_x(T,t) + jR_y(T,t) \tag{24}$$

$$|R(T,t)| = \sqrt{R_x^2(T,t) + jR_y^2(T,t)}$$

$$R(0,t) = \int_{t'=t-nT}^{t'=t} (x^2(t') + y^2(t'))dt'$$

Finally, the results of CFI enter a display encoder and scan conversion whose display properties are implementation dependent. Typically, a color image is overlaid on a standard gray scale image. Colors are chosen to represent blood flow velocity, turbulence, and direction; red is used to indicate flow towards the transducer and blue to represent flow away from it. Green, another primary color, is used to indicate turbulence and the hue of the color is increased as the velocity or intensity is increased.

A variation of CFI, called power Doppler, is often used and is a color representation of Doppler intensity. The display consists of mapping the summation of the magnitude, *R(0, t)*, derived from the complex baseband Doppler signal. The power Doppler is more sensitive to detect presence of blood flow than conventional methods, but provides no information about direction or velocity.

7.3.1 Wall Filter

Wall filter is a high-pass filter used in applications to reduce or eliminate the high-amplitude, low-velocity echoes from vessel walls, also named *wall thump* [23]. The frequency cut-off of the filter is selectable, and, typically, in the range of 50 - 1600 Hz. Even with several challenges in the design, the filter response needs to be very sharp, which necessitates the use of the IIR filter. The filter operates on very few samples (in the order 4 to 16); therefore, there is almost no settling time, so good initialization of the filter is very important. The following are examples of IIR filter initialization [4], [19].

- Zero initialization: The filter states are initialized to zero. This results in poor initial response and is usually not used in ultrasound systems.
- Step initialization: The filter states are calculated on the assumption that the first input to the filter existed since $n = -\infty$ (i.e., for all past time instance).
- Projection initialization: This minimizes the effect of transient response. For second order IIR filter, the filter states are loaded as if the samples with negative time indices had formed a straight line passing through the first two samples of the data sequence to be filtered.

The wall filter can be adaptively chosen based on signal characteristics [29].

8 3D/4D Imaging

Recent advancements in ultrasound imaging include 3D/4D imaging [1], [5], [21]. Note that 4D is simply real-time three-dimensional imaging that varies with time. Major companies have already commercialized such systems and clinical applications are under active research. In this section, a brief introduction of the techniques used in these systems is provided.

8.1 3D Scanning

There are two categories of 3D scanning: mechanical and electronic [1].

- Mechanical: Any transducer used to create 2D B-mode images can be used to acquire slices of 2D images in three dimensions. The mechanical movement can include tilting, rotation or linear displacement. Usually a motorized transducer is used to accurately determine the relative position of the 2D slice being imaged. Figure 12 shows an example of tilting-based acquisition of 2D slices in 3D space.

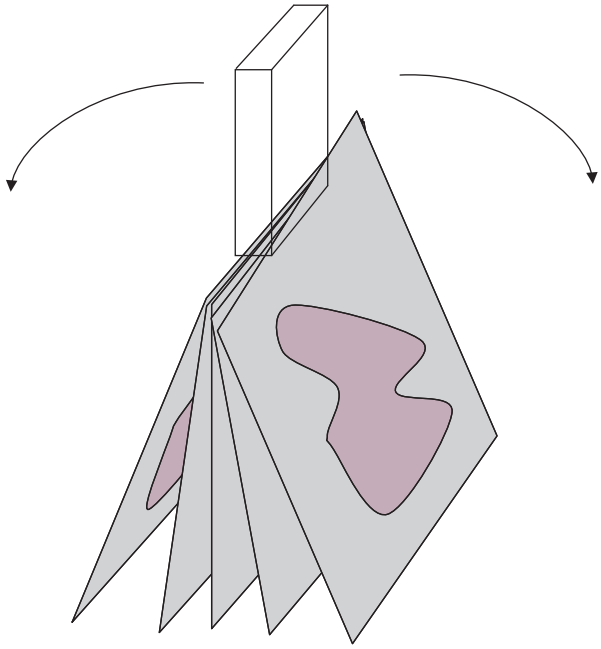

Figure 12. 3D Ultrasound Acquisition Based on Mechanical Tilting of Transducer Assembly

Based on the transducer (linear, curvilinear, phased array, etc.) and movement used (tilting, rotational or linear displacement, etc.), the image is acquired in cylindrical, spherical or Cartesian coordinates.

- Electronic: Figure 13 illustrates an electronic 3D scanning using a full 2D transducer and electronic steering, with beamforming in both azimuth and elevation.

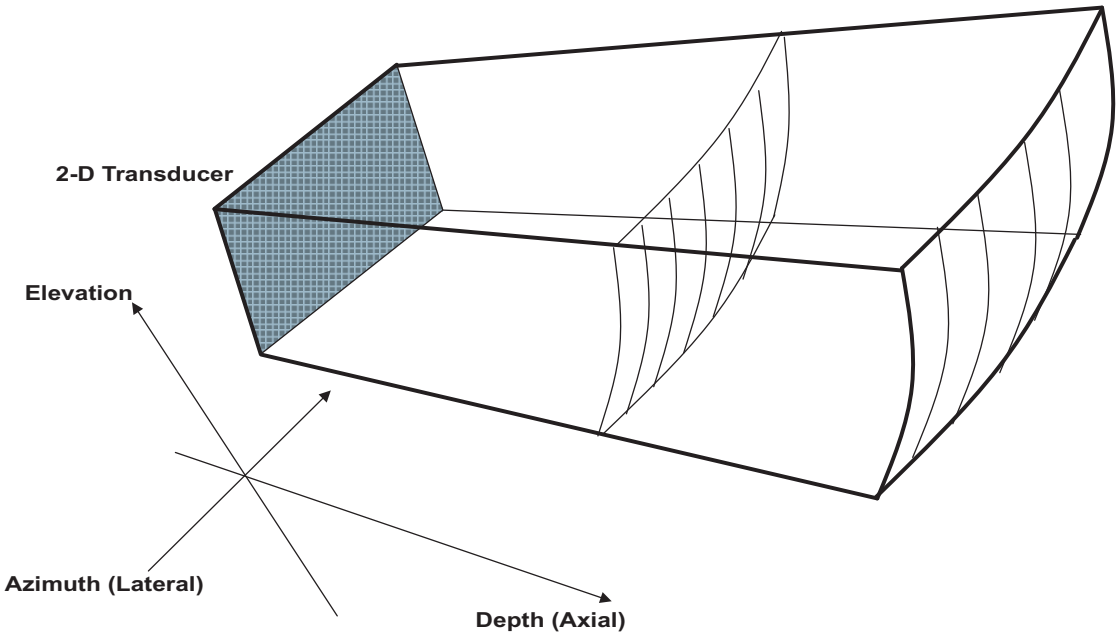

Figure 13. Scanning Using 2D Transducer

Development of the 2D transducer, using either piezo-electric material or through CMUT, continues to be an active area of research. To achieve the desired reliability and yield, several sparse structures for 2D transducer have been proposed in literature [12], [31]. 3D electronic scanning acquires the image in spherical coordinates.

8.2 3D Scan Conversion

The scanning technique determines the coordinate system in which the data is acquired. The 3D volume is internally represented in the Cartesian coordinate system with each point inside a cube representing a voxel of data. Therefore, a conversion of coordinates representing the image is required as shown in Figure 14. This conversion, in its general form, requires trilinear interpolation (e.g, using the 8 nearest neighbors around the desired point).

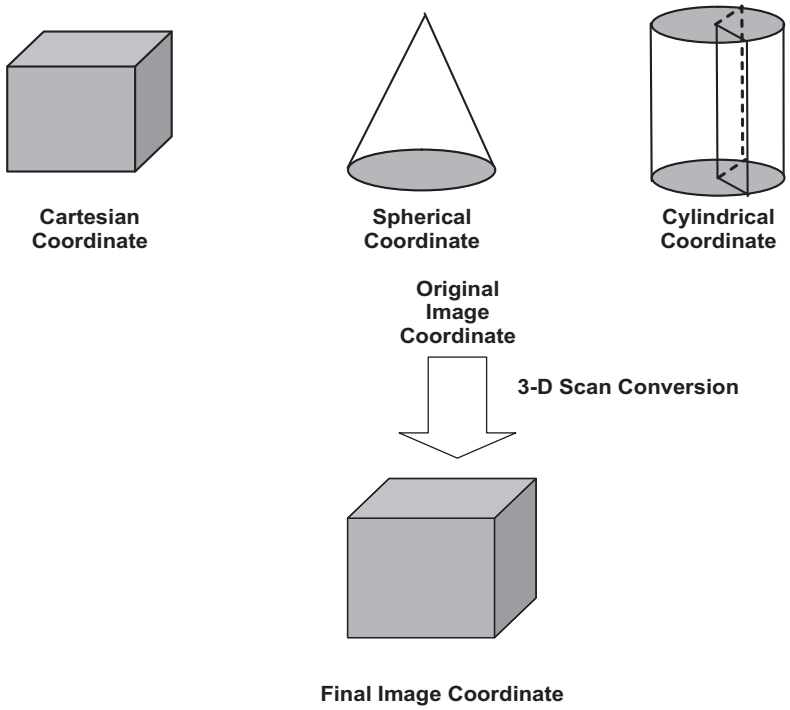

Figure 14. 3D Scan Conversion

8.3 3D Smoothing

Due to speckles, the acquired data is inherently noisy; therefore, smoothing and other image enhancement techniques are often employed. The techniques described in Section 6, can be used on each 2D slice that forms the 3D volume. It is also possible to extend some of these techniques to 3 dimensions. For example, use of 3D Gaussian filtering and median filtering has been reported in literature [1].

8.4 3D Volume Rendering

Once a volume of data is created for viewing, the next step is presenting this data to the physician. There are two techniques of presentation: multi-planar rendering and volume rendering [1], [21].

- Multi-planar rendering (MPR): In this rendering mode, three orthogonal planes are chosen for viewing by the physician as shown in Figure 15. Computer interface is provided so that the user can choose the planes. The values of the pixels on these planes are extracted and presented for display.

- Volume rendering: The most common method of volume rendering is ray casting. In this rendering method, an imaginary ray perpendicular to the plane is drawn through the volume for each pixel in the viewing plane (Figure 16). Since the ray cannot lie exactly on the voxels, trilinear interpolation is usually used to determine the value inside the volume on that ray. The contribution of each point in that ray is then accumulated to determine the overall value of the pixel in the viewing plane. The following methods of accumulation are the most popular for volume rendering.

– Maximum intensity projection (MIP): Only the maximum value along the ray is taken as the value of pixel in the image plane.

– Opacity accumulation: An opacity value, *a(I)*, and a luminance value, *c(I)*. is assigned to every point in the ray. The opacity is usually dependent on the local value of the pixel and luminance on the local gradient. Then, the rendered value along the ray can be calculated as a weighted accumulated sum, which is given below:

$$V(i) = V(i-1)(1-a(i)) + c(i)a(i) \quad (25)$$

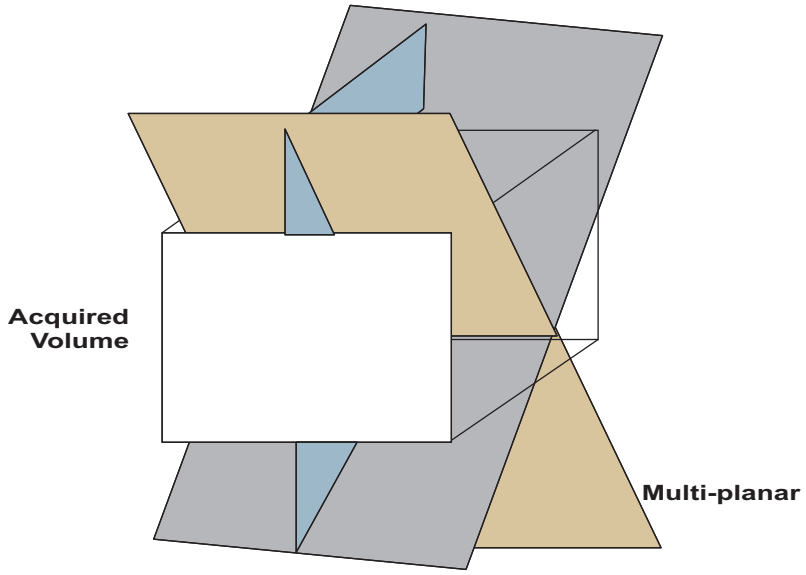

Figure 15. Slices for Multi-Planar Viewing

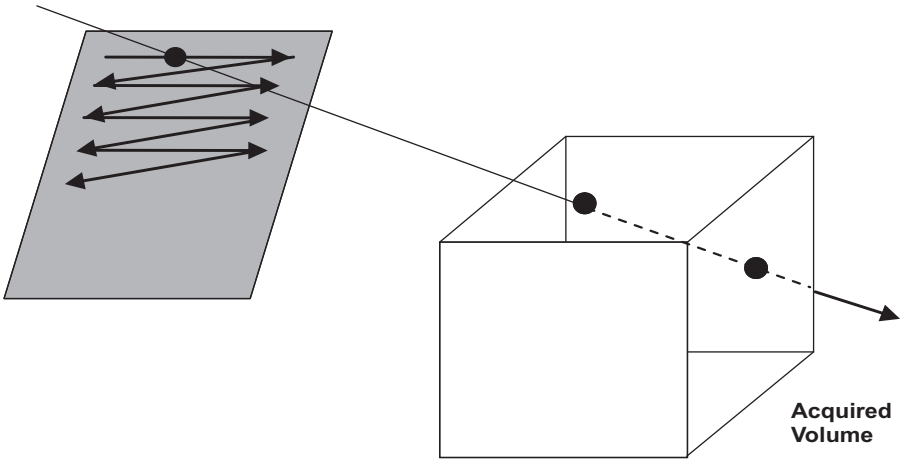

Figure 16. Ray Casting

9 Conclusion

Modern ultrasound systems are signal processing intensive. Advanced techniques of signal processing are used to provide better image quality and higher diagnostic value. New advancements like 3D/4D imaging only increases the processing requirements of such systems. Equipment manufacturers are continuously challenged to bring new functionalities into their systems. Embedded processors, like DSP, provide the manufacturers the capability to maintain similar architecture across device types and generations. In addition, it also provides the ability for field upgradeability to bring in new features on existing equipments. Low-power embedded processors, especially with full system-on-chip capabilities, enable portable battery operated systems. Such portable systems are finding their way into point-of-care applications. With advancement of low-power technologies on the semiconductor side and new algorithms on the processing side, expect ultrasound systems to be more ubiquitous in the future.

10 References

1. *Advanced Signal Processing Handbook: Theory and Implementation for Radar, Sonar, and Medical Imaging Real-Time Systems*, Stergiopoulos, S., ed., CRC Press: Boca Raton, FL, 2001.
2. Abd-Elmoniem, K. Z., Youssef, A. M., and Kadah, Y. M., Real-Time Speckle Reduction and Coherence Enhancement in Ultrasound Imaging via Nonlinear Anisotropic Diffusion, *IEEE Transactions Biomedical Engineering*, Vol. 49, No. 9, pp. 997-1014, September 2002.
3. Averikiou, M. A., Tissue Harmonic Imaging, *Proceedings of the IEEE Ultrasonics Symposium*, pp. 1561-1566, 2000.
4. Biaerum, S., Torp, H, and Kristoffersen, K., Clutter Filter Design for Ultrasound Color Flow Imaging, *IEEE Transactions on Ultrasonics, Ferroelectric, and Frequency Control*, Vol. 49, No. 2, pp. 204-216, February 2002.
5. Fensten, A., and Downey, D. B., 3D Ultrasound Imaging: A review, *IEEE Engineering in Medicine and Biology Magazine*, pp. 41-50, November/December 1996.
6. Fidanzati, P., Morganti, T., and Totoli, P., Real-Time Software Processing and Audio Reproduction of Directional Doppler Signals, *Ultrasound in Medicine and Biology*, Vol. 31, No. 12, pp. 1736-1741, 2005.
7. Kasai, C., Namekawa, K., Koyano, A., and Omoto, R., Real-Time Two-Dimensional Blood Flow Imaging Using an Autocorrelation Technique, *IEEE Transactions on Sonics and Ultrasonics*, Vol. SU-32, No. 3, pp. 458-464, May 1985.
8. Kassam, M. S., Lau, C. W., Cobbold, R. S. C., and Johnston, K. W., Directional CW Doppler Ultrasound Using a Double-Heterodyne Demodulator, *Proceedings of the IEEE Ultrasonics Symposium*, pp. 780-784, 1980.
9. Kim, Y. S., and Ra, J. B., Improvement of Ultrasound Image Based on Wavelet Transform: Speckle Reduction and Edge Enhancement, *Proceedings of SPIE, Medical Imaging: Image Processing*, Vol. 5747, pp. 1085-1092, 2005.
10. Lee, B. B. and Ferguson, E. A., Golay Code for Simultaneous Multi-Mode Operation in Phased Arrays, *Proceedings of the IEEE Ultrasonics Symposium*, pp. 821-825, 1982.
11. Lewis, G.K., Chirped PVDF Transducers for Medical Ultrasound Imaging, *Proceedings of the IEEE Ultrasonics Symposium*, pp. 879-884, 1987.
12. Light, E. D., Mukundan, S., Wolf, P. D., and Smith, S., Real-Time 3D Intracranial Ultrasound with an Endoscopic Matrix Array Transducer, *Ultrasound in Medicine and Biology*, Vol. 33, No. 8, pp. 1277-1284, 2007.
13. Loupas, T., McDicken, W. N., and Allan, P. L., An Adaptive Weighted Median Filter for Speckle Suppression in Medical Ultrasound Images, *IEEE Transactions on Circuits and Systems*, Vol. 36, No. 1, pp. 129-135, January 1989.
14. Loupas, T., Powers, J. T., and Gill, R., An Axial Velocity Estimator for Ultrasound Blood Flow Imaging, based on a Full Evaluation of the Doppler Equation by Means of a Two-Dimensional Autocorrelation Approach, *IEEE Transactions on Ultrasonics, Ferroelectrics, and Frequency Control*, Vo;. 42. No. 4, pp. 672-688, July 1995.
15. Melton, M. E. Jr., Skorton, D. J., Rational Gain Compensation for Attenuation in Utrasonic Cardiac Imaging, *Proceedings of the IEEE Ultrasonics Symposium*, pp. 607-611, 1981.
16. O'Donnel, M., Coded Excitation System for Improving the Penetration of Real Time Phased Array Imaging System, *IEEE Transactions on Utrasonics, Ferroeletrics, and Frequency Control*, Vol. 39, pp. 341-351, 1992.

17. Ophir, J., Garra, B., Kallel, F., Konofagou, E., Krouskop, T., Righetti, R., and Varghese, T., Elastographic Imaging, *Ultrasound in Medicine and Biology*, Vol. 26, Supplement 1, pp. S23-S29, 2000.
18. Parker, K. J., Gao, L., Lerner, R. M., and Levinson, S. F., Techniques for Elastic Imaging: A Review, *IEEE Engineering in Medicine and Biology Magazine*, pp. 52-59, 1996.
19. Peterson, R. B., Atlas, L. E., and Beach, K. W., A Comparison of IIR Initialization Techniques for Improved Color Doppler Wall Filter Performance, *Proceedings of the IEEE Ultrasonics Symposium*, pp. 1705-1708, 1994.
20. Quistgaard, J. U., Signal Acquisition and Processing in Medical Diagnostic Ultrasound, *IEEE Signal Processing Magazine*, pp. 67-74, January 1997.
21. Sakas, G., Schreyer, L. A., and Grimm, M., Preprocessing and Volume Rendering of 3D Ultransonic Data, *IEEE Computer Graphics and Applications*, Vol. 15, No. 4, pp. 47-54, July 1995.
22. Sikdar, S., Managuli, R., Gong, L., Shamdasani, V., Mitake, T., Hayashi, T., and Kim, Y., A Single Mediaprocessor Based Programmable Ultrasound System, *IEEE Transactions of Information Technology in Biomedicine*, Vol 7., No. 1, pp. 64-70, March 2003.
23. Shung K. K., *Diagnostic Ultrasound: Imaging and Blood Flow Measurements*, CRC Press, Taylor and Francis Group: Boca Raton, FL, 2006.
24. Szabo, T. L., *Diagnostic Ultrasound Imaging: Inside Out*, Elsevier Academic Press: Hartford, Connecticut, 2004.
25. Tang, M., and Liu, D., Rationalized Gain Compensation for Ultrasound Imaging, *IFMBE Proceedings of the 7th Asian-Pacific Conference on Medical and Biological Engineering*, Vol. 19, Part 7, pp. 282-285, 2008.
26. Thomenius, Kai E., Evolution of Ultrasound Beamformers, *Proceedings of the IEEE Ultrasonics Symposium*, pp.1615-1922, 1996.
27. Tomasi, C., and Manduchi, R., Bilateral Filtering for Gray and Color Images, *Proceedings of the Sixth International Conference on Computer Vision*, pp. 839-846, 1998.
28. Tupholme, G.E., Generation of Acoustic Pulses by Baffled Plane Pistons, *Mathematika*, Vol.16, pp.209-224, 1969.
29. Yang, M. Y., Managuli, R., and Kim, Y., Adaptive Clutter Filtering for Ultrasound Color Flow Imaging, *Ultrasound in Medicine and Biology*, Vol. 29, No. 9, pp. 1311-1320, 2003.
30. Yang, Z., and Fox, M. D., Speckle Reduction and Structure Enhancement by Multichannel Median Boosted Anisotropic Diffusion, *EURASIP Journal on Applied Signal Processing*, Issue 16, pp. 2492-2502, 2004.
31. Yen, J. T., and Smith, S. W., Real-Time Rectilinear Volumetric Imaging Using a Periodic Array, *Ultrasound in Medicine and Biology*, Vol. 28, No. 7, pp. 923-931, 2002.
32. Zhang, B., and Allebach, J. P., Adaptive Bilateral Filter for Sharpness Enhancement and Noise Removal, *IEEE Transactions on Image Processing*, Vol. 17, No. 5, pp. 664-678, May 2008.
33. Zhuang, X., D.S. Lin, A.S. Ergun, O. Oralkan, B.T. Khuri-Yakub, Trench-Isolated CMUT Arrays With a Supporting Frame, *Proceedings of the IEEE Ultrasonics Symposium*, pp.1995-1958, 2006.
34. Zong, X., Laine, A., and Geiser, E. A., Speckle Reduction and Contrast Enhancement of Echocardiograms via Multiscale Nonlinear Processing, *IEEE Transactions on Medicla Imaging*, Vol. 17, No. 4, pp. 532-540, August 1998.

IMPORTANT NOTICE

Texas Instruments Incorporated and its subsidiaries (TI) reserve the right to make corrections, modifications, enhancements, improvements, and other changes to its products and services at any time and to discontinue any product or service without notice. Customers should obtain the latest relevant information before placing orders and should verify that such information is current and complete. All products are sold subject to TI's terms and conditions of sale supplied at the time of order acknowledgment.

TI warrants performance of its hardware products to the specifications applicable at the time of sale in accordance with TI's standard warranty. Testing and other quality control techniques are used to the extent TI deems necessary to support this warranty. Except where mandated by government requirements, testing of all parameters of each product is not necessarily performed.

TI assumes no liability for applications assistance or customer product design. Customers are responsible for their products and applications using TI components. To minimize the risks associated with customer products and applications, customers should provide adequate design and operating safeguards.

TI does not warrant or represent that any license, either express or implied, is granted under any TI patent right, copyright, mask work right, or other TI intellectual property right relating to any combination, machine, or process in which TI products or services are used. Information published by TI regarding third-party products or services does not constitute a license from TI to use such products or services or a warranty or endorsement thereof. Use of such information may require a license from a third party under the patents or other intellectual property of the third party, or a license from TI under the patents or other intellectual property of TI.

Reproduction of TI information in TI data books or data sheets is permissible only if reproduction is without alteration and is accompanied by all associated warranties, conditions, limitations, and notices. Reproduction of this information with alteration is an unfair and deceptive business practice. TI is not responsible or liable for such altered documentation. Information of third parties may be subject to additional restrictions.

Resale of TI products or services with statements different from or beyond the parameters stated by TI for that product or service voids all express and any implied warranties for the associated TI product or service and is an unfair and deceptive business practice. TI is not responsible or liable for any such statements.

TI products are not authorized for use in safety-critical applications (such as life support) where a failure of the TI product would reasonably be expected to cause severe personal injury or death, unless officers of the parties have executed an agreement specifically governing such use. Buyers represent that they have all necessary expertise in the safety and regulatory ramifications of their applications, and acknowledge and agree that they are solely responsible for all legal, regulatory and safety-related requirements concerning their products and any use of TI products in such safety-critical applications, notwithstanding any applications-related information or support that may be provided by TI. Further, Buyers must fully indemnify TI and its representatives against any damages arising out of the use of TI products in such safety-critical applications.

TI products are neither designed nor intended for use in military/aerospace applications or environments unless the TI products are specifically designated by TI as military-grade or "enhanced plastic." Only products designated by TI as military-grade meet military specifications. Buyers acknowledge and agree that any such use of TI products which TI has not designated as military-grade is solely at the Buyer's risk, and that they are solely responsible for compliance with all legal and regulatory requirements in connection with such use.

TI products are neither designed nor intended for use in automotive applications or environments unless the specific TI products are designated by TI as compliant with ISO/TS 16949 requirements. Buyers acknowledge and agree that, if they use any non-designated products in automotive applications, TI will not be responsible for any failure to meet such requirements.

Following are URLs where you can obtain information on other Texas Instruments products and application solutions:

Products		**Applications**	
Amplifiers	amplifier.ti.com	Audio	www.ti.com/audio
Data Converters	dataconverter.ti.com	Automotive	www.ti.com/automotive
DSP	dsp.ti.com	Broadband	www.ti.com/broadband
Clocks and Timers	www.ti.com/clocks	Digital Control	www.ti.com/digitalcontrol
Interface	interface.ti.com	Medical	www.ti.com/medical
Logic	logic.ti.com	Military	www.ti.com/military
Power Mgmt	power.ti.com	Optical Networking	www.ti.com/opticalnetwork
Microcontrollers	microcontroller.ti.com	Security	www.ti.com/security
RFID	www.ti-rfid.com	Telephony	www.ti.com/telephony
RF/IF and ZigBee® Solutions	www.ti.com/lprf	Video & Imaging	www.ti.com/video
		Wireless	www.ti.com/wireless

Mailing Address: Texas Instruments, Post Office Box 655303, Dallas, Texas 75265